

---

# BENCHMARKING ROBUSTNESS OF CONTRASTIVE LEARNING MODELS FOR MEDICAL IMAGE-REPORT RETRIEVAL

---

Demetrio Deanda Yuktha Priya Masupalli Jeong Yang Young Lee Zechun Cao Gongbo Liang

Department of Computational, Engineering, and Mathematical Sciences  
Texas A&M University-San Antonio

{ddean09, ymasu01}@jaguar.tamu.edu, {jyang, ylee, zcao, gliang}@tamusa.edu

## ABSTRACT

Medical images and reports offer invaluable insights into patient health. The heterogeneity and complexity of these data hinder effective analysis. To bridge this gap, we investigate contrastive learning models for cross-domain retrieval, which associates medical images with their corresponding clinical reports. This study benchmarks the robustness of four state-of-the-art contrastive learning models: CLIP, CXR-RePaiR, MedCLIP, and CXR-CLIP. We introduce an occlusion retrieval task to evaluate model performance under varying levels of image corruption. Our findings reveal that all evaluated models are highly sensitive to out-of-distribution data, as evidenced by the proportional decrease in performance with increasing occlusion levels. While MedCLIP exhibits slightly more robustness, its overall performance remains significantly behind CXR-CLIP and CXR-RePaiR. CLIP, trained on a general-purpose dataset, struggles with medical image-report retrieval, highlighting the importance of domain-specific training data. The evaluation of this work suggests that more effort needs to be spent on improving the robustness of these models. By addressing these limitations, we can develop more reliable cross-domain retrieval models for medical applications.

**Keywords** Trustworthy · AI · Neural Network · Cross-Modality · X-Ray

## 1 Introduction

The rapid growth of medical data, including images and reports, presents both opportunities and challenges for healthcare professionals. While these data sources offer valuable insights into patient health, their heterogeneity, and complexity can hinder effective analysis and decision-making [1]. To bridge this gap, there is a pressing need for AI models capable of jointly understanding both modalities [2].

Cross-domain retrieval, which involves establishing connections between data from distinct sources, has the potential to revolutionize medical research and practice. By combining information from multiple domains, healthcare providers can gain a more comprehensive understanding of patient conditions, leading to more accurate diagnoses and personalized treatment plans [3, 4]. Furthermore, cross-domain retrieval can facilitate the discovery of new medical insights by revealing patterns and trends that might otherwise be obscured. In addition, cross-domain retrieval for medical imaging-report can also facilitate the automated generation of medical imaging reports [5, 6, 7].

Contrastive learning has emerged as a promising technique for cross-domain retrieval in medical imaging and reports [8, 9, 6]. While neural networks have demonstrated impressive performance in various tasks, such as cyber security [10, 11], healthcare [12, 13], public transportation [14, 15], and astrophysics [16, 17, 18], modern neural networks are suffering from issues like miscalibration [19, 20, 21], bias [22], reliability [23], and vulnerability to adversarial attacks [24, 25]. To address these limitations, it is crucial to benchmark the robustness of different models.

This paper investigates the robustness of the contrastive learning-based cross-domain retrieval models, including CLIP [9], CXR-RePaiR [5], MedCLIP [6], and CXR-CLIP [7], for cross-domain retrieval in medical imaging and

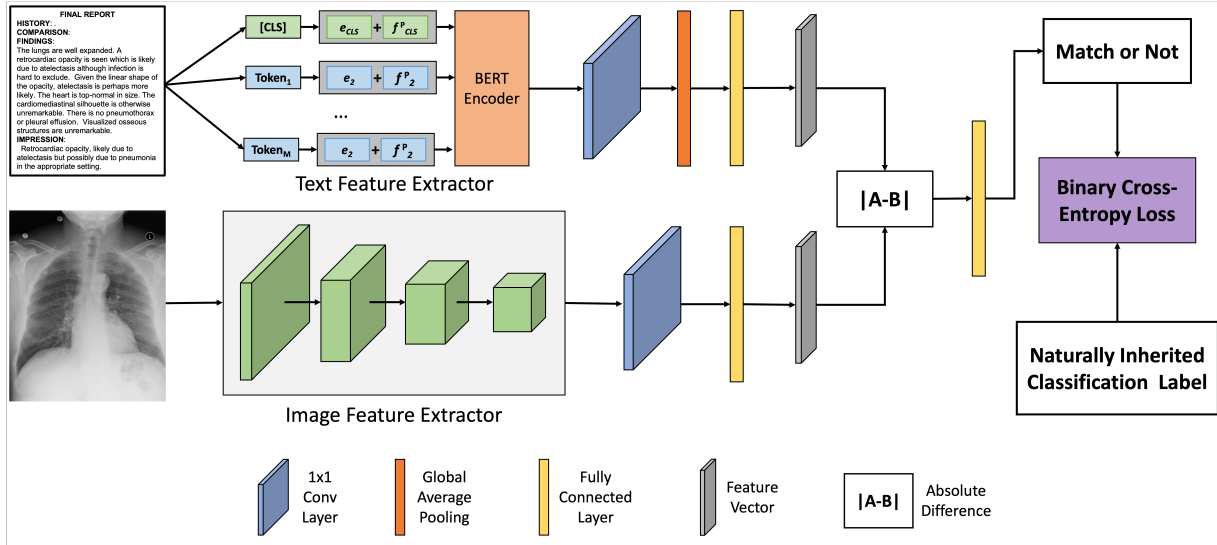


Figure 1: Example of a classification-based contrastive learning model.

reports. By establishing benchmarks, we aim to identify strengths, weaknesses, and potential areas for improvement in future research.

## 2 Problem Definition

In the context of medical imaging, cross-domain retrieval involves associating medical images with their corresponding clinical reports [7, 5]. This task is challenging due to the inherent differences in the nature of these data modalities. However, recent advancements in contrastive learning has enabled significant progress in this area [9, 8].

### 2.1 Contrastive learning

Contrastive learning is a technique that learns general data representations by comparing similar and dissimilar samples. In the imaging domain, Siamese networks, composed of two identical subnetworks, are commonly used for this purpose [26]. These networks process pairs of images and output feature vectors, which are then compared using a loss function like triplet loss [27] or contrastive loss [28, 29]. Alternatively, a binary cross-entropy loss can be used to train Siamese networks as a binary classification problem [30, 31].

To jointly understand medical images and their corresponding reports, a Siamese-style network with distinct subnetworks can be employed. Given a dataset  $X$  of image-text pairs  $\{(I_j, T_k)\}$ , where  $I_j \in \mathcal{I}$  is an image and  $T_k \in \mathcal{T}$ ,  $\mathcal{I}$  and  $\mathcal{T}$  denoting a set of images and a set of textual reports, respectively. If  $j = k$ , the image and report are matching. The goal of contrastive learning is to learn a model  $h(\cdot)$  that pulls the embeddings of matching image-text pairs closer in the feature space and pushes those of non-matching pairs further apart.

The model  $h(\cdot)$  typically consists of two branches:  $h_i(\cdot)$  for processing images and  $h_t(\cdot)$  for processing text. The image branch often employs a convolutional neural network (CNN) or a Vision Transformer (ViT), such as ResNet [32] or Vision Transformer [33], to extract visual features  $v_i$ . The text branch, usually is a large language model (LLM) like BERT [34] or RoBERTa [35], extracts textual features  $v_t$ . These features are then projected to the same space and compared using contrastive losses, such as triplet loss, or classified using a binary classifier.

### 2.2 Contrastive Learning for Cross-Domain Retrieval

Contrastive learning is a powerful technique for training cross-domain retrieval models, which can be employed in two ways: similarity comparison and binary classification.

Contrastive learning brings together samples from the same group (e.g., a matching image and report) in the feature space, while simultaneously pushing apart samples from different groups (e.g., non-matching pairs). This enables

a straightforward approach to retrieval: by comparing the embeddings similarity between images and reports in the feature space. A higher similarity score indicates a stronger match [5, 9].

Alternatively, when a contrastive learning model is trained as a binary classifier, the classification model itself can be directly utilized for retrieval. As illustrated in Figure 1, the model processes an image  $I_j$  through the image processing branch  $h_i(\cdot)$  and a text report  $T_k$  through the text processing branch  $h_t(\cdot)$ . The absolute difference between the resulting embedding vectors,  $v_i$  and  $v_t$ , is fed into a shallow classification model to determine whether the pair is a match. The classification probability can then be used as a retrieval score [8].

### 3 Method

This work investigates the robustness of four contrastive learning models applied to medical image-report retrieval tasks. Given a query image, the objective is to retrieve the most relevant report. This section outlines the detailed evaluation methodology.

#### 3.1 Robustness Evaluation

To assess the robustness of the pre-trained contrastive learning-based cross-domain retrieval methods, we introduced an occlusion retrieval task. During evaluation, we systematically occluded a portion ( $p$ ) of the image ( $p = \{0\%, 0.25\%, 1\%, 4\%, 9\%, 25\%, 49\%, 81\%\}$ ) at random locations, generating out-of-distribution data for the pre-trained models. These occluded images were then used as input to the models for retrieval tasks.

To evaluate the robustness of the models, we calculated  $Recall@k$ , a metric that measures the proportion of relevant items retrieved within the top  $k$  results. We varied the value of  $k$  ( $\{5, 10, 20, 30, 50, 100\}$ ) to assess performance at different retrieval depths.  $Recall@k$  is calculated as follows:

$$Recall@k = \frac{\# \text{ of relevant items retrieved in top } k}{\text{Total \# of relevant items}}. \quad (1)$$

Ideally, a robust model should exhibit similar  $Recall@k$  values across different occlusion levels, especially for smaller occlusion percentages  $p$ .

Algorithm 1 provides a detailed description of occlusion retrieval with a specific occlusion ratio.

#### 3.2 Cross-Domain Retrieval Models

This work evaluates four contrastive learning-based models for cross-domain retrieval tasks: CLIP [9], CXR-RePaiR [5], MedCLIP [6], and CXR-CLIP [7].

##### 3.2.1 CLIP (Contrastive Language-Image Pre-training)

This neural network learns a shared feature space for images and text. Trained on a massive dataset of image-text pairs, CLIP maximizes similarity between semantically related pairs while minimizing it for unrelated ones. This allows CLIP to understand the connection between visual and textual information, enabling tasks like image classification and zero-shot learning. In our work, we leverage CLIP’s learned embeddings for image-text retrieval by calculating cosine similarity between image and text embeddings generated by the pre-trained model.

##### 3.2.2 CXR-RePaiR (Contrastive X-ray-Report Pair Retrieval)

This method generates chest X-ray reports through a retrieval-based fashion. It fine-tuned CLIP on the MIMIC-CXR [36] dataset for report-level or sentence-level retrieval. Report-level retrieval selects the entire best-matching report from the candidate set, while sentence-level retrieval constructs a new report by selecting sentences from multiple reports. For consistency with other methods, we employ the report-level retrieval in this work, calculating cosine similarity between query image embeddings and textual report embeddings generated by a CLIP model that was initialized with CXR-RePaiR weights (available on their official GitHub repository<sup>1</sup>).

##### 3.2.3 MedCLIP

This neural network model is jointly trained on medical images and their corresponding text reports. Unlike previous methods, MedCLIP utilizes unpaired data, reducing the need for large amount of paired data. Designed as a general-purpose medical imaging model, MedCLIP may perform various tasks like zero-shot learning, supervised classification,

<sup>1</sup><https://github.com/rajpurkarlab/CXR-RePaiR>

---

**Algorithm 1** Occlusion Retrieval Test for a Pre-Trained Image-Text Retrieval Model

---

**Require:** Pre-Trained Image-Text Retrieval Model  $h(\cdot)$ , Chest X-Ray Imaging Set  $\mathcal{I}$  with  $M$  images, Textual Report Set  $\mathcal{T}$  with  $N$  reports, Occlusion ratio  $p$  indicating the percentage pixel will be blocked, Constant  $k$  for calculating Recall@ $K$

```

total_correct ← 0                                ▷ The number of relevant report retrieved within the top  $k$  results

for  $m \leftarrow 0$  to  $M - 1$  do                                ▷ For every image
     $i \leftarrow \mathcal{I}[m]$                                 ▷ Get the  $m^{\text{th}}$  chest x-ray image
     $S \leftarrow []$                                 ▷ An empty array holding the matching score between an image and all reports

    for  $n \leftarrow 0$  to  $N - 1$  do                                ▷ For every report
         $t \leftarrow \mathcal{T}[n]$                                 ▷ Get the  $n^{\text{th}}$  report
         $i_o \leftarrow \phi(i, p)$                                 ▷ Generate the occlusion version of  $i$  by random block a  $p\%$  of pixels
         $s \leftarrow h(i_o, t)$                                 ▷ A score indicates the degree of matching between  $i_o$  and  $t$ ,
                                                                ▷ a higher value indicates a better match
         $S.append([t, s])$                                 ▷ Append the report and matching score to the array  $S$ 
    end for

     $S.sort()$                                 ▷ Sort  $S$  according  $s$  in an descending order

    if the corresponding report in the top  $k$  items in  $S$  then                                ▷ If the matched report is in the top
                                                                ▷  $k$  retrieved items
         $total\_correct \leftarrow total\_correct + 1$                                 ▷ Increase the number by 1
    end if

end for

 $recall \leftarrow total\_correct/M$                                 ▷ Calculate Recall@ $K$ 

return  $recall$                                 ▷ Return Recall@ $K$ 

```

---

and image-text retrieval. Here, we focus on its image-text retrieval capabilities. We leverage publicly available code and pre-trained weights from the official MedCLIP GitHub repository<sup>2</sup> in this study.

### 3.2.4 CXR-CLIP

Similar to MedCLIP, CXR-CLIP aims to train a general-purpose image-text model using limited data. However, instead of unpaired data, CXR-CLIP leverages Large Language Models (LLMs) to expand image-label pairs into natural language descriptions. Additionally, it utilizes multiple images and report sections for contrastive learning. To effectively learn image and textual features, CXR-CLIP introduces two novel loss functions: ICL and TCL. ICL focuses on learning study-level characteristics of medical images, while TCL focuses on learning report-level characteristics. Pre-trained CXR-CLIP models can perform both zero-shot learning and image-text retrieval. We evaluate CXR-CLIP’s image-text retrieval capabilities using the official code and pre-trained model available on CXR-CLIP’s official GitHub repository<sup>3</sup>.

### 3.3 MIMIC-CXR Dataset

The MIMIC-CXR dataset [36] is a dataset that widely used for contrastive learning and image-text retrieval in the medical domain. The dataset contains 227,835 radiographic studies from 64,588 patients, encompassing 368,948 chest X-rays and their corresponding radiology reports. The dataset also provides 14 labels (13 for abnormalities and one for normal cases) derived from radiology reports using NLP tools like NegBio [37] and CheXpert [38].

The official validation set includes 2,991 imaging studies, each containing one or more chest X-rays paired with a single textual report (e.g. Figure 2). Each report is divided into sections such as History, Comparison, Findings, and Impression. To ensure data quality, we filtered out reports missing the Findings or Impression sections, resulting in a final validation set of 994 studies with 1,770 X-rays. This filtered dataset is, then, used in our experiments.

---

<sup>2</sup><https://github.com/RyanWangZf/MedCLIP>

<sup>3</sup><https://github.com/Soombit-ai/cxr-clip>



**HISTORY:** \_\_\_-year-old female with chest pain.

**COMPARISON:** Comparison is made with chest radiographs from \_\_\_.

**FINDINGS:** The lungs are well expanded. A retrocardiac opacity is seen which is likely due to atelectasis although infection is hard to exclude. Given the linear shape of the opacity, atelectasis is perhaps more likely. The heart is top-normal in size. The cardiomediastinal silhouette is otherwise unremarkable. There is no pneumothorax or pleural effusion. Visualized osseous structures are unremarkable.

**IMPRESSION:** Retrocardiac opacity, likely due to atelectasis but possibly due to pneumonia in the appropriate setting.

Figure 2: Example of a chest x-ray (left) with the radiology report (right) from the MIMIC-CXR dataset [36].

	Method	Occlusion Area in Percentage								Random Performance
		0.00%	0.25%	1.00%	4.00%	9.00%	25.00%	49.00%	81.00%	
Recall @ 5	CLIP	0.57	0.45	0.51	0.40	0.51	0.40	0.62	0.45	0.50
	CXR-RePaiR	14.76	14.54	13.69	13.35	10.24	5.43	1.36	0.45	
	CXR-CLIP	48.56	47.26	46.92	43.47	37.42	20.41	5.94	0.34	
	MedCLIP	1.19	1.24	1.30	1.19	1.02	0.73	0.62	0.40	
Recall @ 10	CLIP	1.07	1.07	0.90	0.90	0.85	0.79	1.07	0.85	0.99
	CXR-RePaiR	23.47	22.45	22.45	20.31	16.86	8.54	2.83	0.74	
	CXR-CLIP	58.68	57.66	58.06	52.63	46.24	27.93	9.84	1.13	
	MedCLIP	2.37	2.43	2.54	2.77	2.09	1.69	1.36	0.96	
Recall @ 20	CLIP	2.04	1.98	1.81	1.75	1.75	1.75	1.81	1.70	2.01
	CXR-RePaiR	34.05	34.05	33.37	29.36	25.34	13.63	4.47	1.36	
	CXR-CLIP	67.55	67.44	65.86	61.56	56.08	38.33	15.43	1.98	
	MedCLIP	4.46	4.63	4.24	3.95	4.12	3.33	2.71	1.64	
Recall @ 30	CLIP	3.00	3.00	2.71	2.71	2.71	2.83	3.11	2.38	3.02
	CXR-RePaiR	40.61	39.93	38.97	36.26	32.24	17.65	5.60	1.87	
	CXR-CLIP	73.21	71.91	71.34	67.55	61.39	43.75	19.45	3.00	
	MedCLIP	5.82	6.10	6.05	5.59	5.88	4.75	3.73	2.66	
Recall @ 50	CLIP	5.20	4.81	4.36	4.58	4.24	4.36	5.54	4.13	5.03
	CXR-RePaiR	49.66	49.21	48.59	45.31	41.57	24.77	9.39	3.96	
	CXR-CLIP	79.48	78.58	78.58	74.51	67.83	52.80	28.21	5.48	
	MedCLIP	9.21	8.98	9.38	8.47	8.93	7.51	6.21	4.52	
Recall @ 100	CLIP	10.07	9.39	9.11	9.56	9.11	9.56	9.45	8.60	9.94
	CXR-RePaiR	64.03	64.14	62.73	59.39	56.17	37.84	18.27	8.54	
	CXR-CLIP	88.19	87.73	87.51	84.17	79.54	66.76	40.53	11.42	
	MedCLIP	16.50	16.61	17.23	16.16	16.27	14.29	12.82	9.83	

Table 1: Occlusion retrieval results of all the models at various occlusion ratio (from 0% to 81%)

## 4 Result

### 4.1 Cross-Domain Retrieval

Table 1 presents the occlusion retrieval results of the four evaluated models for various occlusion percentages. **Bold text** highlight the best performance for each occlusion ratio and recall threshold. **Blue text** indicates the second-best performance, while **red text** denotes the worst performance.

The table reveals that CXR-CLIP consistently achieves the best performance across most occlusion ratios and recall thresholds, except for the 81% occlusion level for Recall@5. CXR-RePaiR consistently achieves the second-best performance for all occlusion ratios, except for the 81% occlusion level. MedCLIP generally ranks third, but it achieves the second-best performance five times at the 81% occlusion level across six different recall thresholds. CLIP consistently performs the worst, with most results aligning with random performance.

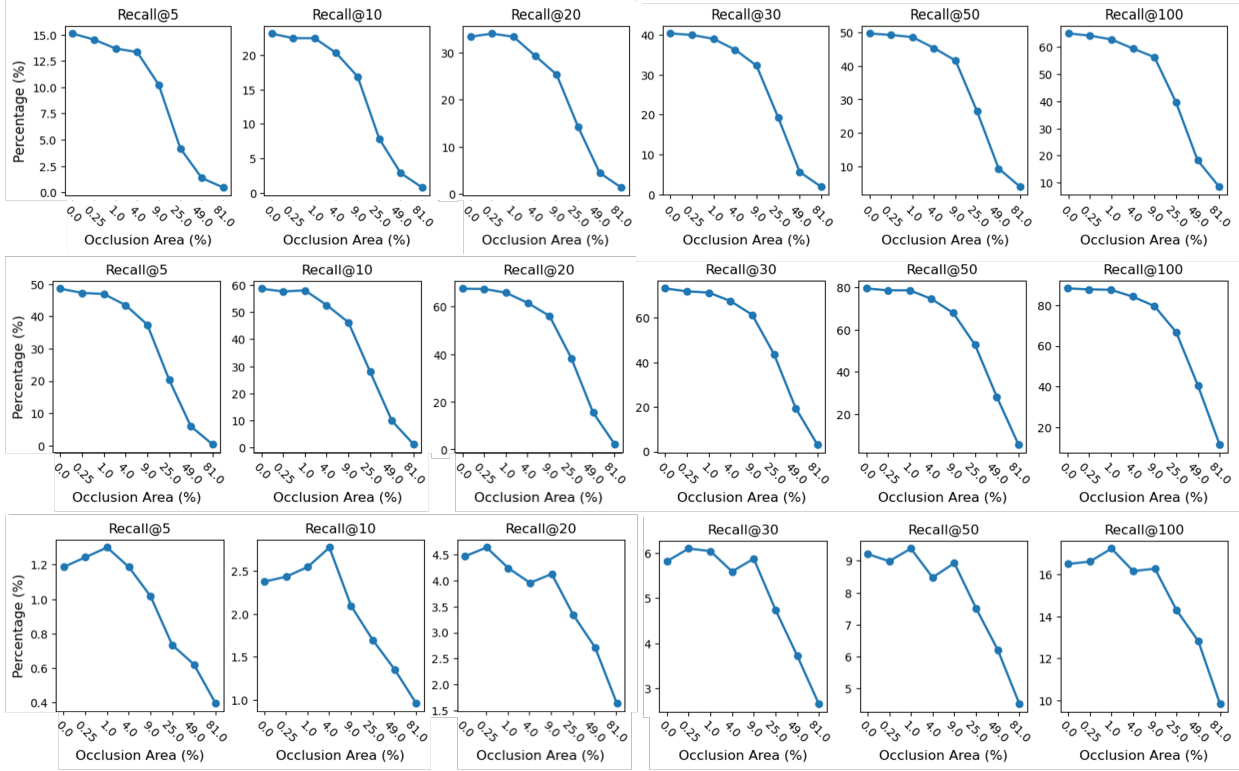


Figure 3: Robustness testing result for CXR-RePaiR (top), CXR-CLIP (middle), and ViT-based MedCLIP (bottom).

While CLIP’s poor performance is expected due to its training on natural images, MedCLIP’s relatively weaker performance is surprising, given its training on medical data. However, this aligns with the performance trends reported in the MedCLIP paper, where MedCLIP outperforms CLIP by approximately two times [6]. We believe MedCLIP’s weaker retrieval performance stems from its integration of unpaired images, texts, and labels using a rule-based labeler, which may hinder the model’s ability to accurately associate images with their corresponding reports due to the decoupling of image-text pairs.

## 4.2 Robustness Analysis

Figure 3 visualizes the performance of CXR-RePaiR (Figure 3 top), CXR-CLIP (Figure 3 middle), and MedCLIP (Figure 3 bottom), respectively. All three models exhibit a decrease in performance as the image occlusion percentage increases. The performance degradation is generally proportional to the occlusion level, with MedCLIP showing a slightly slower decline (approximately 20%) compared to the other two models. This near-proportional performance decrease suggests that none of the models are robust to handle occluded or out-of-distribution data.

Between CXR-RePaiR and CXR-CLIP, CXR-RePaiR shows a slightly steeper decline in performance, indicating lower robustness compared to CXR-CLIP.

While MedCLIP exhibits a weaker overall retrieval performance, its slower decline in performance suggests potential robustness. Especially for low occlusion levels (less than 4%), slight occlusions may even improve MedCLIP’s retrieval performance. We hypothesize that this is due to the model’s training on unpaired images, texts, and labels. Slight occlusions may act as a form of noise reduction, smoothing out potential overfitting and improving generalization.

## 5 Conclusion

This study investigates the robustness of contrastive learning-based cross-domain retrieval models for medical image-report retrieval tasks. By introducing an occlusion retrieval task, we assessed the performance of CLIP, CXR-RePaiR, MedCLIP, and CXR-CLIP under varying levels of image corruption.

Our findings indicate that CXR-CLIP consistently outperforms the other models, demonstrating superior retrieval performance. CXR-RePaiR exhibits the second-best performance, while MedCLIP, despite its potential, shows a weaker overall performance, especially in the presence of significant occlusions. CLIP, trained on a general-purpose dataset, struggles with medical image-report retrieval, highlighting the importance of domain-specific training data.

However, all the evaluated models are extremely sensitive to out-of-distribution data, as shown by the proportional decrease in performance with increasing occlusion percentages. While MedCLIP might exhibit slightly more robustness, its overall performance remains behind CXR-CLIP and CXR-RePaiR. We hypothesize that this is due to its training on unpaired images, texts, and labels. Slight occlusions may act as a form of noise reduction, improving generalization. However, the decoupling of image-text pairs in the unpaired training setting may limit the model’s ability to accurately associate images with their corresponding reports.

Future research should explore techniques to improve the robustness of contrastive learning models. Additionally, investigating the impact of different types of data augmentation and architectural modifications on model performance is crucial. By addressing these limitations, we can develop more robust and reliable cross-domain retrieval models for medical applications.

## Acknowledgment

This material is based upon work supported by the National Science Foundation’s Grant No. 2334243. Any opinions, findings, and conclusions or recommendations expressed in this material are those of the author(s) and do not necessarily reflect the views of National Science Foundation.

## References

- [1] C. S. Kruse, R. Goswamy, Y. J. Raval, and S. Marawi, “Challenges and opportunities of big data in health care: a systematic review,” *JMIR medical informatics*, vol. 4, no. 4, p. e5359, 2016.
- [2] B. Pandey, D. K. Pandey, B. P. Mishra, and W. Rhmann, “A comprehensive survey of deep learning in the field of medical imaging and medical natural language processing: Challenges and research directions,” *Journal of King Saud University-Computer and Information Sciences*, vol. 34, no. 8, pp. 5083–5099, 2022.
- [3] H. M. Yang, T. Duan, D. Ding, A. Bagul, C. Langlotz, K. Shpanskaya *et al.*, “Chexnet: radiologist-level pneumonia detection on chest x-rays with deep learning,” *arXiv preprint arXiv:1711.05225*, 2017.
- [4] Q. Ying, X. Xing, L. Liu, A.-L. Lin, N. Jacobs, and G. Liang, “Multi-modal data analysis for alzheimer’s disease diagnosis: An ensemble model using imagery and genetic features,” in *2021 43rd Annual International Conference of the IEEE Engineering in Medicine & Biology Society (EMBC)*. IEEE, 2021, pp. 3586–3591.
- [5] M. Endo, R. Krishnan, V. Krishna, A. Y. Ng, and P. Rajpurkar, “Retrieval-based chest x-ray report generation using a pre-trained contrastive language-image model,” in *Machine Learning for Health*. PMLR, 2021, pp. 209–219.
- [6] Z. Wang, Z. Wu, D. Agarwal, and J. Sun, “Medclip: Contrastive learning from unpaired medical images and text,” in *The 2022 Conference on Empirical Methods in Natural Language Processing*. ACL, 2022.
- [7] K. You, J. Gu, J. Ham, B. Park, J. Kim, E. K. Hong, W. Baek, and B. Roh, “Cxr-clip: Toward large scale chest x-ray language-image pre-training,” in *International Conference on Medical Image Computing and Computer-Assisted Intervention*. Springer, 2023, pp. 101–111.
- [8] G. Liang, C. Greenwell, Y. Zhang, X. Xing, X. Wang, R. Kavuluru, and N. Jacobs, “Contrastive cross-modal pre-training: A general strategy for small sample medical imaging,” *IEEE Journal of Biomedical and Health Informatics*, vol. 26, no. 4, pp. 1640–1649, 2021.
- [9] A. Radford, J. W. Kim, C. Hallacy, A. Ramesh, G. Goh, S. Agarwal, G. Sastry, A. Askell, P. Mishkin, J. Clark *et al.*, “Learning transferable visual models from natural language supervision,” in *International conference on machine learning*. PMLR, 2021, pp. 8748–8763.
- [10] J. Zulu, B. Han, I. Alsmadi, and G. Liang, “Enhancing machine learning based sql injection detection using contextualized word embedding,” in *Proceedings of the 2024 ACM Southeast Conference*, 2024, pp. 211–216.
- [11] G. Liang, J. Guerrero, F. Zheng, and I. Alsmadi, “Enhancing neural text detector robustness with  $\mu$  attacking and rr-training,” *Electronics*, vol. 12, no. 8, p. 1948, 2023.
- [12] X. Xing, G. Liang, C. Wang, N. Jacobs, and A.-L. Lin, “Self-supervised learning application on covid-19 chest x-ray image classification using masked autoencoder,” *Bioengineering*, vol. 10, no. 8, p. 901, 2023.

- [13] L. Liu, J. Chang, G. Liang, and S. Xiong, “Simulated quantum mechanics-based joint learning network for stroke lesion segmentation and tici grading,” *IEEE Journal of Biomedical and Health Informatics*, 2023.
- [14] R. Jonnala, G. Liang, J. Yang, and I. Alsmadi, “Potential and challenges of large language models in public transportation: San antonio case study,” in *the Thirty-Ninth AAAI Conference on Artificial Intelligence (AAAI) Workshop*, 2025.
- [15] G. Liang, J. Zulu, X. Xing, and N. Jacobs, “Unveiling roadway hazards: Enhancing fatal crash risk estimation through multiscale satellite imagery and self-supervised cross-matching,” *IEEE Journal of Selected Topics in Applied Earth Observations and Remote Sensing*, vol. 17, pp. 535–546, 2024.
- [16] J. ZuHone, D. Barnes, N. Jacobs, W. Forman, P. Nulsen, R. Kraft *et al.*, “A deep learning view of the census of galaxy clusters in illustrisng,” *Monthly Notices of the Royal Astronomical Society*, vol. 498, no. 4, pp. 5620–5628, 2020.
- [17] Y. Zhang, G. Liang, Y. Su, and N. Jacobs, “Multi-branch attention networks for classifying galaxy clusters,” in *2020 25th International Conference on Pattern Recognition (ICPR)*. IEEE, 2021, pp. 9643–9649.
- [18] S.-C. Lin, Y. Su, G. Liang, Y. Zhang, N. Jacobs, and Y. Zhang, “Estimating cluster masses from sdss multiband images with transfer learning,” *Monthly Notices of the Royal Astronomical Society*, vol. 512, no. 3, pp. 3885–3894, 2022.
- [19] C. Guo, G. Pleiss, Y. Sun, and K. Q. Weinberger, “On calibration of modern neural networks,” in *International conference on machine learning*. PMLR, 2017, pp. 1321–1330.
- [20] G. Liang, Y. Zhang, X. Wang, and N. Jacobs, “Improved trainable calibration method for neural networks on medical imaging classification,” in *British Machine Vision Conference (BMVC)*, 2020.
- [21] B. Han, Y. Masupalli, X. Xing, and G. Liang, “Multi-scale probabilistic embedding for vision model calibration,” in *2024 IEEE International Conference on Big Data (Big Data)*. IEEE, 2024, pp. 4472–4478.
- [22] X. Wang, G. Liang, Y. Zhang, H. Blanton, Z. Bessinger, and N. Jacobs, “Inconsistent performance of deep learning models on mammogram classification,” *Journal of the American College of Radiology*, vol. 17, no. 6, pp. 796–803, 2020.
- [23] E. Xing, L. Liu, X. Xing, Y. Qu, N. Jacobs, and G. Liang, “Neural network decision-making criteria consistency analysis via inputs sensitivity,” in *2022 26th International Conference on Pattern Recognition (ICPR)*. IEEE, 2022, pp. 2328–2334.
- [24] G. Bortsova, C. González-Gonzalo, S. C. Wetstein, F. Dubost, I. Katramados, L. Hogeweg, B. Liefers, B. van Ginneken, J. P. Pluim, M. Veta *et al.*, “Adversarial attack vulnerability of medical image analysis systems: Unexplored factors,” *Medical Image Analysis*, vol. 73, p. 102141, 2021.
- [25] Y. Zhang, G. Liang, T. Salem, and N. Jacobs, “Defense-pointnet: Protecting pointnet against adversarial attacks,” in *2019 IEEE International Conference on Big Data (Big Data)*. IEEE, 2019, pp. 5654–5660.
- [26] Y. Taigman, M. Yang, M. Ranzato, and L. Wolf, “Deepface: Closing the gap to human-level performance in face verification,” in *Proc. IEEE Conf. Comput. Vis. Pattern Recogn.*, 2014, pp. 1701–1708.
- [27] F. Schroff, D. Kalenichenko, and J. Philbin, “Facenet: A unified embedding for face recognition and clustering,” in *Proc. IEEE Conf. Comput. Vis. Pattern Recogn.*, 2015, pp. 815–823.
- [28] T. Chen, S. Kornblith, M. Norouzi, and G. Hinton, “A simple framework for contrastive learning of visual representations,” in *International conference on machine learning*. PMLR, 2020, pp. 1597–1607.
- [29] K. He, H. Fan, Y. Wu, S. Xie, and R. Girshick, “Momentum contrast for unsupervised visual representation learning,” in *Proceedings of the IEEE/CVF Conference on Computer Vision and Pattern Recognition*, 2020, pp. 9729–9738.
- [30] G. Koch, R. Zemel, and R. Salakhutdinov, “Siamese neural networks for one-shot image recognition,” in *ICML deep learning workshop*, vol. 2. Lille, 2015.
- [31] W. Yang, J. Li, F. Fukumoto, and Y. Ye, “Mscnn: A monomeric-siamese convolutional neural network for extremely imbalanced multi-label text classification,” in *Proceedings of the 2020 Conference on Empirical Methods in Natural Language Processing (EMNLP)*, 2020, pp. 6716–6722.
- [32] K. He, X. Zhang, S. Ren, and J. Sun, “Deep residual learning for image recognition,” in *Proceedings of the IEEE conference on computer vision and pattern recognition*, 2016, pp. 770–778.
- [33] A. Dosovitskiy, “An image is worth 16x16 words: Transformers for image recognition at scale,” *arXiv preprint arXiv:2010.11929*, 2020.



- [34] J. D. M.-W. C. Kenton and L. K. Toutanova, “Bert: Pre-training of deep bidirectional transformers for language understanding,” in *Proceedings of naacL-HLT*, vol. 1. Minneapolis, Minnesota, 2019, p. 2.
- [35] Y. Liu, “Roberta: A robustly optimized bert pretraining approach,” *arXiv preprint arXiv:1907.11692*, vol. 364, 2019.
- [36] A. E. Johnson *et al.*, “Mimic-cxr, a de-identified publicly available database of chest radiographs with free-text reports,” *Scientific data*, vol. 6, no. 1, pp. 1–8, 2019.
- [37] Y. Peng, X. Wang, L. Lu, M. Bagheri, R. Summers, and Z. Lu, “Negbio: a high-performance tool for negation and uncertainty detection in radiology reports,” in *Proc. AMIA Summits on Trans. Sci.*, 2018.
- [38] J. Irvin *et al.*, “Chexpert: A large chest radiograph dataset with uncertainty labels and expert comparison,” in *Proc. AAAI Conf. on Artif. Intel.*, 2019.